



XXI International Polish-Slovak Conference “Machine Modeling and Simulations 2016

## Modeling of a sintering process at various scales

Jerzy Rojek<sup>\*</sup>, Szymon Nosewicz, Marcin Maździarz, Piotr Kowalczyk,  
Krzysztof Wawrzyk, Dmytro Lumelskyj

*Institute of Fundamental Technological Research, Polish Academy of Sciences, Pawińskiego 5B, 02-106 Warsaw, Poland*

---

### Abstract

This paper presents modeling of a sintering process at various scales. Sintering is a powder metallurgy process consisting in consolidation of powder materials at elevated temperature but below the melting point. Sintering models at the atomistic, microscopic and macroscopic scales have been presented. Sintering is a process governed by diffusion therefore the atomistic modeling using the molecular dynamics has been focused on investigation of the diffusion process. The micromechanical model has been developed within the framework of the discrete element method. It allows us to consider microstructure and its changes during sintering. The macroscopic model is based on the continuum phenomenological approach. It combines elastic, thermal and viscous creep deformation. The methodology to determine macroscopic quantities: stress, strains and constitutive viscous properties from the discrete element simulations has been presented. Possibilities of the developed models have been demonstrated by applying them to simulation of sintering of the intermetallic NiAl powder. Own experimental results have been used to calibrate and validate numerical models.

© 2017 The Authors. Published by Elsevier Ltd. This is an open access article under the CC BY-NC-ND license (<http://creativecommons.org/licenses/by-nc-nd/4.0/>).

Peer-review under responsibility of the organizing committee of MMS 2016

*Keywords:* sintering; modeling; discrete element method; diffusion; molecular dynamics; macroscopic model;

---

### 1. Introduction

Sintering is a technique of powder metallurgy in which solid parts are manufactured from metal or ceramic powder mixtures. Sintering consists in consolidation of loose or weakly bonded powders at elevated temperatures, close to the melting temperature with or without additional pressure. During sintering a particulate material is converted into a solid compact body. At the macroscopic level, one can observe a change of the mechanical

---

<sup>\*</sup> Corresponding author. Tel.: (+48) 22 826 12 81 147.  
E-mail address: [jrojek@ippt.pan.pl](mailto:jrojek@ippt.pan.pl)

properties (a material acquires a certain mechanical strength), a change of geometry and volume (shrinkage) and an increase of bulk density (due to shrinkage).

The macroscopic changes result from processes undergoing at the microscopic level. Figure 1 shows a microstructure of the intermetallic NiAl at an early stage of sintering. The microstructure during sintering undergoes an evolution characterized by grain rearrangement and increase of grain compaction. In the initial stage, cohesive bonds (necks) are formed between powder particles. When the sintering process is continued the necks between particles grow due to mass transport. Surface and grain boundary diffusion are normally dominant mechanisms of mass transport in sintering. The stresses in the neck and the surface tension induce particle attraction, which leads to shrinkage of the system. The neck growth and shrinkage conduct to the reduction and sometimes to the practical elimination of material porosity.

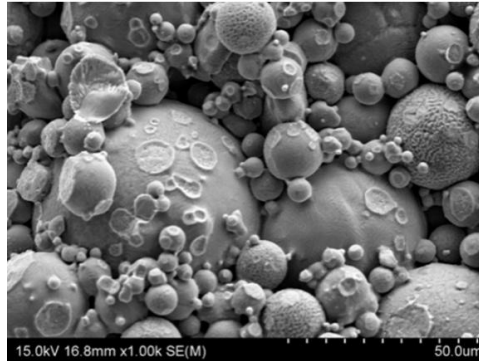


Fig. 1. Microstructure of NiAl at an early stage of sintering.

Sintering is a complex process and the quality of the sintered components depends on many factors, cf. [1]. Numerical modeling can predict evolution of a sintering process and possible defects of sintered parts, thus helping to design and optimize the process. Sintering phenomena can be modelled at various scales. Different sintering models are reviewed in [2–5].

The present paper will present numerical models of sintering phenomena at three scales: atomistic, microscopic and macroscopic ones. Connections and transitions between the models at different scales will be described. Analysis of a real sintering process of the intermetallic NiAl powder will demonstrate capabilities of the developed models and formulations.

## 2. Atomistic modeling of sintering phenomena

There have been attempts to simulate directly particle sintering using the molecular dynamics, e.g. [6], but such simulations are limited to nanoparticles. Typical particle diameter in such simulations reaches a few nanometers while the particle diameter in the considered NiAl powder is three orders of magnitude larger. Atomistic simulations of sintering of such particles would require enormous computational effort. Therefore atomic and atomistic simulations of sintering mechanisms are usually aimed at determining the diffusivity of a given material system. Similarly, the present work is focused at studies of diffusion as the main mechanism of sintering. The main objective of these studies is to estimate parameters for the micromechanical particle-based model of NiAl sintering.

The solid state sintering is modelled in the present work, thus, the diffusion occurring in solids is studied. Diffusion in solids is very slow, however, at elevated temperatures, it gets much faster. The sintering temperature is usually in the range 0.7–0.9 of the melting point, high enough for an intensive diffusion.

In the continuum approach, intensity of a stationary diffusion process is described by the Fick's law:

$$\mathbf{J} = -D\nabla n \quad (1)$$

where  $\mathbf{J}$  is the diffusion flux,  $n$  is the scalar concentration field,  $\nabla n$  is the concentration-gradient vector, and  $D$  is the diffusion coefficient of the considered species. The form of Eq. (1) is valid for diffusion in isotropic media. The

diffusion flux is given by the number of particles passing through a unit area per unit time (it has the dimension [ $\text{m}^{-2}\text{s}^{-1}$ ]), the concentration  $n$  is defined as the number of particles per unit volume in [ $\text{m}^{-3}$ ], and consequently, the diffusion coefficient is given in [ $\text{m}^2\text{s}^{-1}$ ].

Diffusion in crystalline solids occurs by atomic hops in a lattice, either to an interstitial position (interstitial diffusion) or to a neighbouring vacancy (vacancy diffusion). The energy necessary for an elementary jump is called the activation energy  $Q$ . The activation energy is an important parameter characterizing diffusion. The diffusion coefficient  $D$  is often expressed by an Arrhenius-type relationship:

$$D = D_0 \exp\left(\frac{-Q}{k_B T}\right) \quad (2)$$

where  $D_0$  is the pre-exponential factor,  $T$  is the absolute temperature and  $k_B$  is the Boltzmann's constant. The relationship given by Eq. (2) predicts that the lower the activation energy and the higher temperature are, the higher the diffusivity is. The diffusivity enters directly as a parameter in the definition of the micromechanical model of sintering.

Diffusion data can be obtained experimentally but this is neither easy nor cheap. In some cases, complete information is almost impossible to get. Therefore, possibility to simulate diffusion process at the atomistic level is important. Molecular Dynamics (MD) provides a straightforward technique to calculate the diffusivity. Since a diffusion process is mediated by a certain type of point defects, the defects are created in the simulation block, and their random walk through the model is enabled by a sufficiently long MD run. The coefficient of diffusion can be calculated from the Einstein-Smoluchowski relation [7] either in the average form:

$$D_{avg.} = \frac{1}{2d} \lim_{x \rightarrow \infty} \frac{\langle [r(t_0 + t) - r(t_0)]^2 \rangle}{t}, \quad (3)$$

or in the instantaneous one:

$$D_{inst.} = \frac{1}{2d} \lim_{x \rightarrow \infty} \frac{\partial \langle [r(t_0 + t) - r(t_0)]^2 \rangle}{\partial t}, \quad (4)$$

where,  $d$  is the dimensionality ( $d = 3$  for volume,  $d = 2$  for surface and grain-boundary diffusion);  $t$  is the time and  $\langle [r(t_0 + t) - r(t_0)]^2 \rangle$  is the ensemble average mean-squared displacement (MSD).

### 3. Micromechanical model of sintering

A number of sintering models have been developed within the discrete element method (DEM), e.g. [8–12]. The discrete element models consider a powder during sintering as a collection of spherical particles (discrete elements) interacting with one another. This enables consideration of a microstructure of a powder material and its changes during sintering.

This work employs the authors' own original viscoelastic model implemented in the in-house DEM code [13]. The particle interaction model in this model is an extension of the particle sintering model developed originally by [14] and [15]. The two-particle model of sintering [14, 15] is derived considering diffusion as the main mechanism of sintering. By analysis of mass transport and stresses at the grain boundary between two sintered particles the following equation for the particle interaction during sintering is obtained:

$$F_n = \frac{\pi t^4}{8D_{eff}} v_m + \pi \gamma_s \left[ 4r \left( 1 - \cos \frac{\Psi}{2} \right) + a \sin \frac{\Psi}{2} \right] \quad (5)$$

where  $F_n$  is the normal force between two particles,  $v_m$  – the normal relative velocity,  $r$  – the particle radius,  $a$  – the radius of the interparticle boundary,  $\Psi$  – the dihedral angle,  $\gamma_s$  – the surface energy. The geometrical parameters of the model are defined in Fig. 2 The value of diffusion parameter directly depends on certain diffusion mechanism, which is considered at the constitutive model of sintering. Assuming that the grain boundary diffusion is a dominant mechanism in the neck growth and shrinkage of the system the effective grain boundary diffusion coefficient  $D_{eff}$  is given by the following formula:

$$D_{\text{eff}} = \frac{D_{\text{gb}} \delta \Omega}{k_B T} \quad (6)$$

where  $D_{\text{gb}}$  is the grain boundary diffusion coefficient with the width  $\delta$ ,  $\Omega$  is the atomic volume,  $k_B$  is the Boltzmann constant and  $T$  is the temperature. The model takes into account the thermal expansion – the particle radius  $r$  is calculated as follows:

$$r = r_0(1 + \alpha(T - T_0)) \quad (7)$$

where  $T_0$  is the reference temperature,  $r_0$  is the particle radius at the reference temperature and  $\alpha$  is the linear thermal expansion coefficient. The rate of radius change due to thermal expansion is taken into account in calculation of the normal relative velocity  $v_m$ .

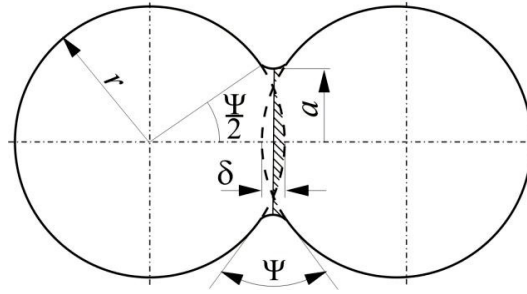


Fig. 2. Two-particle model of sintering.

High computational cost is one of the main drawbacks of the discrete element method which impedes its wider use in engineering practice. Therefore it is important to combine the DEM with a more efficient continuous macroscopic approach. In the present work, the results of the discrete elements simulations will be used to determine macroscopic viscous properties used in the formulation of the macroscopic model of sintering.

#### 4. Macroscopic model of sintering

The macroscopic model of sintering used in this work combines the elastic, thermal and viscous deformation induced by external loading and sintering driving stress. The strain rate  $\dot{\boldsymbol{\epsilon}}$  is decomposed into the elastic, thermal and viscous parts,  $\dot{\boldsymbol{\epsilon}}^e$ ,  $\dot{\boldsymbol{\epsilon}}^T$  and  $\dot{\boldsymbol{\epsilon}}^v$  respectively:

$$\dot{\boldsymbol{\epsilon}} = \dot{\boldsymbol{\epsilon}}^e + \dot{\boldsymbol{\epsilon}}^T + \dot{\boldsymbol{\epsilon}}^v \quad (8)$$

The thermal strain rate is given for isotropic material by:

$$\dot{\boldsymbol{\epsilon}}^T = \alpha \dot{T} \mathbf{I} \quad (9)$$

where  $\alpha$  is the coefficient of linear thermal expansion and  $\mathbf{I}$  is the identity tensor.

The constitutive equation can be written as follows:

$$\dot{\boldsymbol{\sigma}} = \mathbf{C} : (\dot{\boldsymbol{\epsilon}}^e - \dot{\boldsymbol{\epsilon}}^T - \dot{\boldsymbol{\epsilon}}^v) + \mathbf{I} \dot{\boldsymbol{\sigma}}^{\text{sint}} \quad (10)$$

where  $\boldsymbol{\sigma}$  is the Cauchy stress tensor,  $\mathbf{C}$  – the elastic stiffness tensor,  $\boldsymbol{\sigma}^{\text{sint}}$  – the sintering driving stress. Employing the decomposition of the stresses and strain rates in the viscous element into the deviatoric and volumetric parts the relationship between the stress and viscous strain rate can be written as follows [16]:

$$\boldsymbol{\sigma} = \text{dev}(\boldsymbol{\sigma}) + \sigma_m \mathbf{I} = 2\eta_s \text{dev}(\dot{\boldsymbol{\epsilon}}^v) + \eta_v \text{tr}(\dot{\boldsymbol{\epsilon}}^v) \mathbf{I} + \mathbf{I} \sigma^{\text{sint}} \quad (11)$$

where  $\sigma_m$  is the mean stress

$$\sigma_m = \frac{\text{tr}(\sigma)}{3} \tag{12}$$

and  $\eta_s$  and  $\eta_v$  are the shear and volumetric viscous moduli, respectively. The inverse relationship can be easily obtained in the following form:

$$\dot{\epsilon}^v = \text{dev}(\dot{\epsilon}^v) + \frac{\text{tr}(\dot{\epsilon}^v)}{3} \mathbf{I} = \frac{\text{dev}(\sigma)}{2\eta_s} + \frac{\sigma_m - \sigma^{\text{sint}}}{3\eta_v} \tag{13}$$

In the phenomenological modeling, constitutive model parameters are obtained by fitting experimental data. The present work will show an alternative way to determine the macroscopic properties of a sintered material based on the simulation of sintering process at a lower, microscopic, scale.

First, macroscopic strains and stresses will be obtained by averaging over representative volume elements [17, 18]. Then, assuming that the constitutive relationships (11) and (13) are valid for the effective averaged stresses and strains the macroscopic moduli can be evaluated as follows:

$$\eta_s = \frac{\|\text{dev}(\sigma)\|}{2\|\text{dev}(\dot{\epsilon}^v)\|}, \quad \eta_v = \frac{\sigma_m - \sigma^{\text{sint}}}{\text{tr}(\dot{\epsilon}^v)} \tag{14}$$

where the symbol  $\|\cdot\|$  denotes the norm of a second order tensor – for the deviatoric parts of the stress and viscous strain tensors the norms are defined as follows:

$$\|\text{dev}(\sigma)\| = (\text{dev}(\sigma) : \text{dev}(\sigma))^{\frac{1}{2}}, \quad \|\text{dev}(\dot{\epsilon}^v)\| = (\text{dev}(\dot{\epsilon}^v) : \text{dev}(\dot{\epsilon}^v))^{\frac{1}{2}}. \tag{15}$$

## 5. Numerical results

Numerical models described above have been applied to simulation of a sintering process of the NiAl powder. Sintering of the NiAl at temperature of 1673 K under uniaxial pressure of 30 MPa has been investigated in our laboratory (see Fig. 1). Diffusivity parameters estimated by molecular dynamics simulations have been used in the discrete element simulation of sintering as initial data. The final values of micromechanical parameters have been established by fitting the numerical evolution of the relative density with the experimental results. Finally, discrete element simulations have been used to determine macroscopic constitutive properties.

### 5.1. Estimation of diffusivity for NiAl by molecular dynamics simulations

Diffusion process in the NiAl in the temperature range from 1573 to 1673 K (corresponding to the sintering temperature in laboratory tests) has been studied using the MD program LAMMPS (Large-scale Atomic/Molecular Massively Parallel Simulator) [19]. The embedded-atom method potential EAM2009 [20] has been used in the atomistic model. The quality of this potential has been assessed checking the melting point temperature predicted by the potential and a set of parameters such as the lattice constant, cohesive energy, elastic constants, bulk modulus, surface energy, defect energies, migration energies calculated for NiAl by molecular statics approach [21, 22].

The grain boundary diffusion has been investigated using the models representing bicrystals of NiAl with different crystal orientations shown in Fig. 3. Grain boundary diffusivity for different bicrystals are shown in the form of the Arrhenius plot in Fig. 4. The numerical values of diffusion parameters are given in Table 1. The results confirm that the grain boundary diffusivity depends on the relative monocrystal orientation.

Table 1. Grain-boundary diffusivity results.

| Bicrystal type | $D_{0b}$ [m <sup>2</sup> /s] | $Q$ [kJ/mol] |
|----------------|------------------------------|--------------|
| [100 - 110]    | $3.66 \cdot 10^{-7}$         | 208          |
| [100 - 111]    | $1.94 \cdot 10^{-5}$         | 214          |
| [110 - 111]    | $1.73 \cdot 10^{-5}$         | 218          |

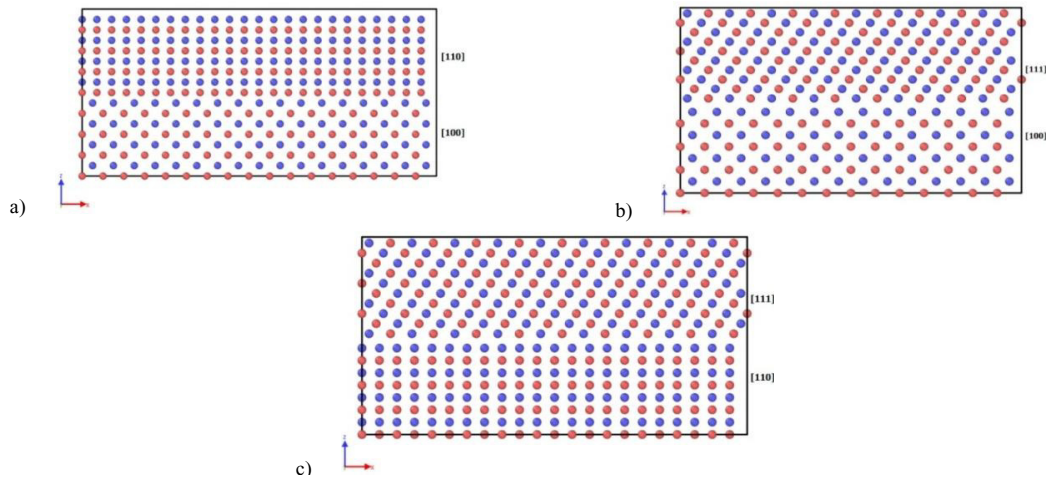


Fig. 3. Atomistic models for simulation of grain boundary diffusion in NiAl bicrystal.

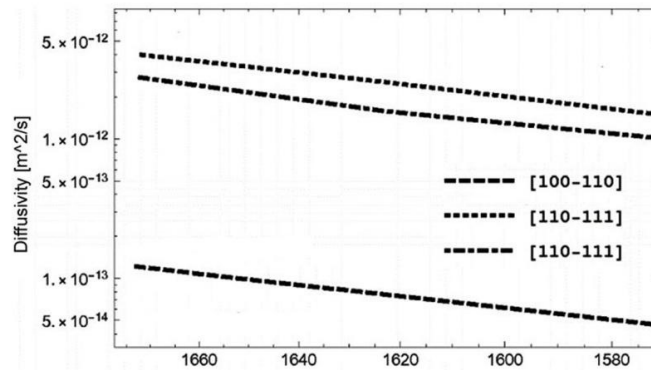


Fig. 4. Diffusivity Arrhenius plot.

## 5.2. Discrete element simulation of sintering

Laboratory tests of sintering of the NiAl powder have been simulated using the discrete element model. Experimental tests have been performed under pressure of 30 MPa and at temperature of 1673 K. The simulations have been performed using the DEM model formed by 1751 particles filling a cylinder with fixed walls confining the powder subject to uniaxial compression by a plate representing the punch. The initial configuration of the particle assembly before pressing is shown in Fig. 5a.

The model has been created maintaining the original size (mean particle radius 3.97 μm) and size distribution of powder particles and taking a reduced diameter (200 μm) of a cylinder confining the powder. It has been assumed that such a reduced geometric model represents correctly sintering process in a real specimen with diameter of 120 mm. This assumption is justified provided the material behavior is uniform in the real specimen volume.

The specimen geometry at different stages of simulation can be seen in Fig. 5. Figure 5b shows the geometry of the specimen under pressure of 30 MPa before heating. The final geometry of the sintered specimen is presented in Fig. 5c. A significant height reduction in the process of sintering can be observed. The volumetric shrinkage is associated with the changes of the bulk density.

Initial analysis of sintering has been performed assuming the average diffusivity data from the MD simulations:  $D_{0b} = 1.24 \cdot 10^{-5} \text{ m}^2/\text{s}$ ,  $Q = 213 \text{ kJ/mol}$ . Figure 6 shows the numerical density evolution curve in comparison with experimental data. It can be seen that the numerical simulation with initial diffusivity parameters has predicted a slower densification. The experimental data have been matched taking the pre-exponential factor of the grain boundary diffusion  $D_{0b}$  as the fitting parameter. A good agreement with experimental results has been obtained taking  $D_{0b} = 9 \cdot 10^{-5} \text{ m}^2/\text{s}$ ,  $Q = 213 \text{ kJ/mol}$ .

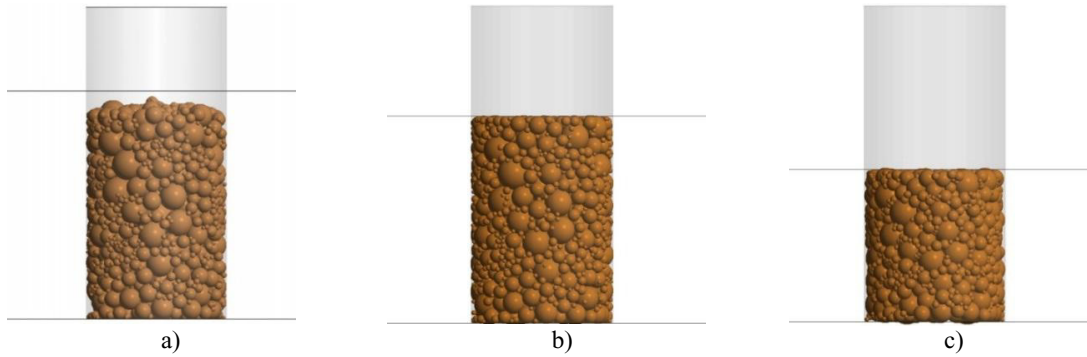


Fig. 5. DEM simulation of sintering: a) specimen before pressing, b) specimen after pressing and before sintering, c) specimen after sintering.

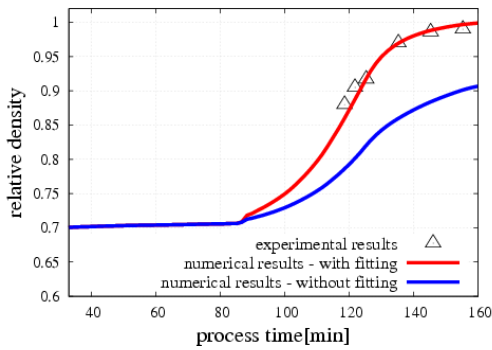


Fig. 6. Evolution of the relative density during the process – comparison of numerical and experimental results.

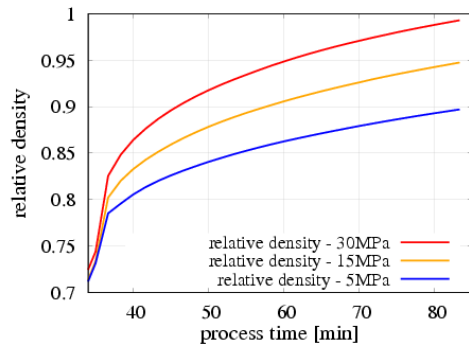


Fig. 7. Evolution of the relative density for different pressures.

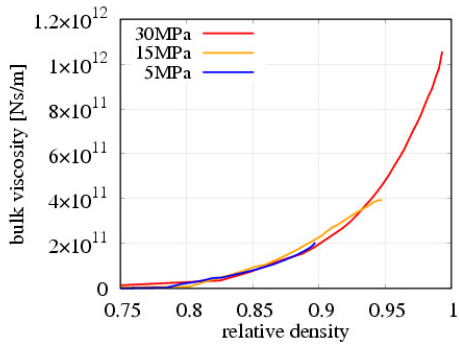


Fig. 8. Bulk viscous modulus as a function of the relative density.

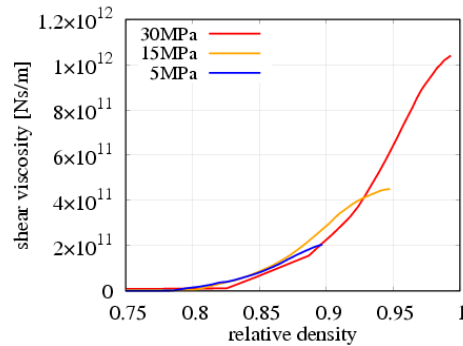


Fig. 9. Shear viscous modulus as a function of the relative density.

### 5.3. Determination of macroscopic viscous moduli

The DEM model with diffusivity parameters determined in the previous section has been used in simulations specially conceived to give macroscopic viscous moduli of the sintered material. For this purpose, the simulations of NiAl sintering have been carried out for the temperature 1673 and three values of uniaxial pressure: 5, 15 and 30 MPa. The evolution of the relative density during the whole process is plotted in Fig. 7. Using the methodology described in Sec. 4 the macroscopic viscous moduli have been determined. The bulk and shear viscous moduli obtained for different pressure levels have been plotted as functions of the relative density in Figs. 8 and 9, respectively. It can be easily noticed that the curves corresponding to different pressures coincide very well. This confirms correctness of our simulations. The micromechanical model does not assume any pressure dependence of the constitutive parameters and this is reflected in the macroscopic constitutive properties. It can be seen from Figs.

8 and 9 that the numerical calculations predict an increase of the viscous moduli with increasing density. This increase becomes faster when the relative density tends to unity.

## 6. Conclusions

Possibilities of modeling of sintering phenomena have been presented. Modeling at the atomistic scale using the molecular dynamics enables estimation of the diffusivity parameters which can be used in the micromechanical particle model of sintering. The diffusivity parameters require certain fitting to match numerical and experimental results. Micromechanical discrete element simulations can be used to determine macroscopic constitutive properties. The presented models and inter-scale transitions form a framework for multiscale modeling of sintering.

## Acknowledgements

This project has been financed from the funds of Polish National Science Centre (NCN) awarded by decision numbers DEC-2013/11/B/ST8/03287.

## References

- [1] M. Chmielewski, D. Kaliński, K. Pietrzak, and W. Włosiński. Relationship between mixing conditions and properties of sintered 20AlN/80Cu composite materials. *Archives of Metallurgy and Materials*, 55 (2010) 579–585.
- [2] J.-M. Missiaen. Modelling of sintering: recent developments and perspectives. *Rev. Met. Paris*, 12 (2002) 1009–1019.
- [3] J. Pan. Modelling sintering at different length scales. *International Materials Reviews*, 2,17 (2003) 69–85.
- [4] H.E. Exner and T. Kraft. Review on computer simulations of sintering processes. In *Powder Metallurgy World Congress 2*, 1998, pp. 278–283, EPMA, Shrewsbury, U.K.
- [5] D. Gendron. Etude numerique et experimentale du frittage a lechelle du grain. PhD thesis, L'Universite Bordeaux I, 2001.
- [6] Brian J. Henz, Takumi Hawa, and Michael Zachariah. Molecular dynamics simulation of the kinetic sintering of Ni and Al nanoparticles. *Molecular Simulation*, 35 (2009) 804–811.
- [7] H. Mehrer. *Diffusion in Solids - Fundamentals, Methods, Materials, Diffusion-Controlled Processes*. Springer, 2007.
- [8] F. Parhami and R.M. McMeeking. A network model for initial stage sintering. *Mechanics of Materials*, 27 (1998) 111–124.
- [9] C.L. Martin, L.C.R. Schneider, L. Olmos, and D. Bouvard. Discrete element modeling of metallic powder sintering. *Scripta Materialia*, 55 (2006) 425–428.
- [10] B. Henrich, A. Wonisch, T. Kraft, M. Moseler, and H. Riedel. Simulations of the influence of rearrangement during sintering. *Acta Materialia*, 55 (2007) 753–762.
- [11] A. Wonisch, T. Kraft, M. Moseler, and H. Riedel. Effect of different particle size distributions on solid-state sintering: A microscopic simulation approach. *J. Am. Ceram. Soc.*, 92 (2009) 1428–1434.
- [12] S. Martin, M. Guessasma, J. Lechelle, J. Fortin, K. Saleh, and F. Adenot. Simulation of sintering using a Non Smooth Discrete Element Method. Application to the study of rearrangement. *Computational Materials Science*, 84 (2014) 31–39.
- [13] S. Nosewicz, J. Rojek, K. Pietrzak, and M. Chmielewski. Viscoelastic discrete element model of powder sintering. *Powder Technology*, 246 (2013) 157–168.
- [14] R.L. Coble. Sintering of Crystalline Solids. Intermediate and Final State Diffusion Models. *J. Appl. Phys.*, 32(1961) 787–792.
- [15] D.L. Johnson. New method of obtaining volume, grain boundary, and surface diffusion coefficients from sintering data. *J. Appl. Phys.*, 40 (1969) 192–200.
- [16] V.V. Skorokhod, E.A. Olevisky, and M.B. Shtern. Continuum Theory for Sintering of Porous Bodies: Model and Application. *Science of Sintering*, 32 (1991) 79–91.
- [17] K. Bagi. Analysis of microstructural strain tensors for granular assemblies. *Int. J. Solids & Structures*, 43 (2006) 3166–3184.
- [18] S. Luding. Micro-macro transition for anisotropic, frictional granular packings. *Int. J. Solids & Structures*, 41, (2004) 5821–5836.
- [19] S. Plimpton. Fast Parallel Algorithms for Short-Range Molecular Dynamics. *J. Comp. Physics*, 117 (1995) 1–19.
- [20] G.P. Purja Pun and Y. Mishin. Development of an interatomic potential for the Ni-Al system. *Philosophical Magazine*, 89 (2009) 3245–3267.
- [21] M. Maździarz, T.D. Young, and G. Jurczak. A study of the affect of prerelaxation on the nanoindentation process of crystalline copper. *Archives of Mechanics*, 63, 2011, pp. 533.
- [22] M. Maździarz, T.D. Young, P. Dłużewski, T. Wejrzanowski, and K.J. Kurzydłowski. Computer modelling of nanoindentation in the limits of a coupled molecular–statics and elastic scheme. *J. Comp. Theor. Nanosci.*, 7, 2010, pp. 1172.